Catalysis
Science & Technology

RSC Publishing

COMMUNICATION

View Article Online
View Journal | View Issue

Cite this: *Catal. Sci. Technol.*, 2013, **3**, 1905

Received 16th January 2013,
Accepted 6th May 2013

DOI: 10.1039/c3cy00041a

www.rsc.org/catalysis

Choosing a suitable support for Co_3O_4 as an NH_3 oxidation catalyst†

Wing-Kin Fung, Leshego Ledwaba, Ngokoana Modiba, Michael Claeys and Eric van Steen*

Co_3O_4 as an NH_3-oxidation catalyst may transform reversibly to CoO under reaction conditions, even in the presence of excess oxygen. The use of alumina may then result in the formation of cobalt aluminate rendering the catalyst inactive. The formation of cobalt aluminate can be avoided by using $ZnAl_2O_4$ as a support.

Introduction

Ammonia oxidation yielding NO/NO_2 forms the core of the nitric acid production plant. This process typically uses a platinum–rhodium gauze as a catalyst for ammonia oxidation, since it is active and highly selective.[1] However, the lifetime of the platinum gauze is rather short (up to 12 months for operation at atmospheric pressure, and the lifetime decreases with increasing reaction pressure).[2] Thus a variety of transition metal oxides for the oxidation of ammonia yielding nitrogen oxides have been studied.[3] Co_3O_4 is utilized in some nitric acid plants[4] and seems to have the added advantage of lower yield of the undesirable greenhouse gas N_2O and longer catalyst lifetime.

Ammonia oxidation is thought to proceed *via* a Mars–van Krevelen mechanism utilizing lattice oxygen.[5,6] Hence, the catalytically active phase in Co_3O_4-catalyzed ammonia oxidation may be reduced to CoO, and this phase transformation may result in catalyst deactivation. The more stable perovskite $LaCoO_3$ has been investigated[6–8] as an alternative. This may however result in a lower intrinsic catalytic activity, due to its resistance to the release of lattice oxygen. Another alternative would be to adapt the reaction conditions (oxygen partial pressure/temperature/crystallite size of Co_3O_4 – *vide verde*) to minimize the reduction of Co_3O_4 under the operating conditions.

The removal of lattice oxygen and re-oxidation are crucial steps in the Mars–van Krevelen mechanism.[5,6] The completion of the catalytic cycle requires the oxidation of CoO, *viz.* $3CoO + \frac{1}{2}O_2 \rightarrow Co_3O_4$. The thermodynamic feasibility of this process is dependent on temperature, partial pressure of oxygen and the crystallite size of Co_3O_4 in the starting material (due to the difference in the surface energy contribution[9]) and in the absence of sintering the thermodynamic feasibility of the re-oxidation process can be expressed as:

$$RT\ln\left(p_{O_2}^{0.5}\right) = \mu^0_{Co_3O_4} - 3\mu^0_{CoO} - \frac{1}{2}\mu^0_{O_2} + \frac{6\gamma_{Co_3O_4}}{d_{Co_3O_4}\underline{\rho}_{Co_3O_4}}\left(1 - \frac{\gamma_{CoO}}{\gamma_{Co_3O_4}}\left(\frac{3\underline{\rho}_{Co_3O_4}}{\underline{\rho}_{CoO}}\right)\right)$$

The surface energy for Co_3O_4 is experimentally determined[10] to be 1.96 J m^{-2} (in reasonable agreement with the estimated surface energy using DFT+U[11]). The reported experimental value for the surface energy of CoO[12] is 2.8 J m^{-2}. However, the theoretical values for the surface energy of CoO are lower than the surface energy of Co_3O_4, *viz.* 0.46 J m^{-2} based on a classical model[9] and 0.79 J m^{-2} using DFT+U for CoO calculated as the anti-ferromagnetic phase AFMII.[13] A higher surface energy of CoO than that of Co_3O_4 implies that the reduction of Co_3O_4 will be thermodynamically impeded for small crystallites, *i.e.* the transition temperature for the transformation of Co_3O_4 to CoO will increase with decreasing crystallite size of Co_3O_4. However, the auto-reduction of supported Co_3O_4[14] shows a lowering in the transition temperature in comparison to unsupported Co_3O_4 implying a lower surface energy of CoO in comparison to Co_3O_4. Fig. 1 shows the predicted dependency of the predicted transition of CoO to Co_3O_4 as a function of the reaction temperature and oxygen partial pressure. The re-oxidation of CoO is expected to be thermodynamically more feasible at low temperatures, high oxygen partial pressures and with large crystallites of Co_3O_4. However, high temperatures are required for ammonia oxidation to minimize N_2O formation.[15] Hence, an operating window for Co_3O_4catalyzed NH_3 oxidation can be defined in terms of temperature, pressure and crystallite size of Co_3O_4.

Centre for Catalysis Research, Department of Chemical Engineering, University of Cape Town, Private Bag X3, Rondebosch 7701, South Africa. E-mail: eric.vansteen@uct.ac.za; Fax: +27 (0)21 650 5501; Tel: +27 (0)21 650 3796

† Electronic supplementary information (ESI) available. See DOI: 10.1039/c3cy00041a

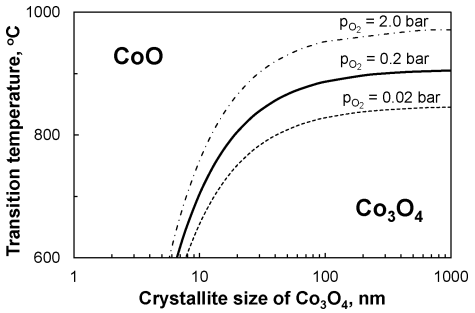

Fig. 1 Predicted thermodynamic transition temperature for the re-oxidation of CoO to Co_3O_4 as a function of the initial crystallite size of Co_3O_4 and the partial pressure of oxygen ($\gamma_{Co_3O_4}$ = 1.96 J m^{-2}; γ_{CoO} = 0.46 J m^{-2}; $\underline{\rho}_{Co_3O_4}$ = 25.2 kmol m^{-3}; $\underline{\rho}_{CoO}$ = 81.6 kmol m^{-3}).

In industrial operation, Co_3O_4 as an ammonia oxidation catalyst is typically used in the form of catalyst pellets resulting in severe mass transfer limitations.[15] The use of smaller pellets in conjunction with the high linear velocity typically employed in the ammonia oxidation would result in a high pressure drop. Hence, it is desirable to incorporate the catalytically active component in a structured reactor (*e.g.* monolith).[8,16] The strong hydrothermal conditions prevalent during ammonia oxidation may result in the formation of the Co-support compound.[17,18] The formation of such compounds would represent a thermodynamic sink. In this communication, we evaluate the activity of Co_3O_4 supported on alumina and zinc aluminate focusing on the possible formation of Co-support compounds. Alumina as a support may result in the formation of $CoAl_2O_4$, if Co_3O_4 is reduced to Co(II)O. However, the formation of $CoAl_2O_4$ is thermodynamically not feasible from Co(II)O and $ZnAl_2O_4$.

Experimental

γ-Al_2O_3 (Degussa; d_{pellet} = 3 mm; S_{BET} = 225 m^2 g^{-1}; V_{pore} = 0.63 cm^3 g^{-1}; d_{pore} = 9 nm) and zinc aluminate were used as support materials. Zinc aluminate was prepared by co-precipitation.[19] The resulting product was pressed into pellets with an average size of 3 mm. An industrial, unsupported Co_3O_4 catalyst (ρ_{pellet} = 3.54 g cm^{-3}; S_{BET} = 0.3 m^2 g^{-1}; V_{pore} = 0.12 cm^3 g^{-1}) containing an irregular distribution of Co_3O_4 crystallites ranging from 200 nm to 5 mm, with the smaller crystallites attached to the large crystallites, was used for comparison.

The support pellets were impregnated with a solution containing $Co(NO_3)_2{\cdot}6H_2O$ in deionised water.[20] The catalyst precursor was aged at room temperature for 20 minutes and dried at 120 °C for 2 hours. Subsequently, the dried precursor was calcined in air (180 ml (STP) min^{-1}) at 350 °C for 2 hours (heating rate: 5 °C min^{-1}). Catalyst pellets were crushed to a size between 125 and 212 μm for the activity test.

The Co_3O_4 loading was verified using AAS-ICP. The BET surface area and micro-pore volume was determined using N_2 adsorption–desorption at 77 K using a Micromeritics Tristar 3000. The phase composition on the catalyst and the average crystallite size of the various phases in the catalyst pellet were determined using X-ray diffraction (Bruker D8 Advance laboratory X-ray diffractometer; source Co-$K_{\alpha,1}$; voltage: 35 kV; current: 40 mA) equipped with a position sensitive detector (VANTEC-2000, Bruker AS). The obtained diffraction patterns were fitted using Rietveld refinement as employed in TOPAS 4.2 (Bruker AXS), such that the weighted profile factor (R_{WP}) was <10 and the Bragg factor (R_{Bragg}) was <5.

The catalytic activity of the catalysts in the ammonia oxidation was determined in a quartz, fixed bed reactor (d_{inner} = 9 mm; d_{outer} = 12 mm, l = 410 mm) with an isothermal zone of 20 mm (ΔT < 5 °C). The catalyst (d_p = 125–212 μm; m = 3 mg) was diluted with *ca.* 300 mg silicon carbide (d_p < 75 μm) and loaded into the isothermal zone. The high degree of dilution ($m_{diluent}$/$m_{catalyst}$ = 100) may result in an inhomogeneous distribution of the catalyst and bypassing of the reactants,[21] however the use of fines as a diluent mitigates this effect, due to extensive radial mixing. A bed of silicon carbide (d_p = 425–600 μm; l = 125 mm) served as a pre-heating zone. A quartz thermo-well (d_{outer} = 4 mm) was inserted into the catalyst bed to monitor the reaction temperature. A pre-mixed gas containing 7.4% NH_3, 19.4% O_2 and the balance He was passed over the catalyst bed at a volumetric flow rate of 100 ml (NTP) min^{-1}. Ammonia oxidation was performed at atmospheric pressure in the temperature range 450–800 °C. The reactor temperature was raised to 450 °C and after 30 minutes the ammonia conversion was determined by bubbling the effluent gas for 20 minutes through deionised water ensuring complete absorption of ammonia. Subsequently, the reactor temperature was raised to investigate the activity at higher temperatures, *viz.* 580 and 740 °C. In order to test the reversibility of the observed deactivation the reactor temperature was subsequently decreased to 580 °C and 450 °C. The concentration of ammonia in the ammonia trap was determined at each reaction temperature spectro-photometrically using the Nessler method[22] (Jenway 6405 UV/Vis spectrometer; λ = 450 nm). The repeatability of the experiments was good and deviations in the ammonia conversion on repeat runs were less than 2%.

The small amount of catalyst used to evaluate the activity does not allow for a post-mortem analysis of the spent catalyst. Hence, the catalyst was used in the form of pellets to enable the characterization of the 'spent' catalyst. The use of pellets introduces mass transfer limitations,[15] which should be kept in mind when interpreting the data. The catalyst pellets (300 mg) were loaded in the isothermal zone of the reactor. The void spaces were filled with *ca.* 300 mg silicon carbide (d_p < 75 μm) to ensure sufficient radial mixing.

Results and discussion

The unsupported Co_3O_4 as a powder shows the normal increase in the ammonia conversion with increasing temperature (see Fig. 2). A further increase in the ammonia conversion is obtained upon the subsequent decrease in temperature. In order to explore this phenomenon better an unsupported Co_3O_4 pellet was loaded (which showed significant internal mass transfer limitations[15]). The ammonia conversion increases with increasing temperature up to 640 °C, after which a decrease in the activity is observed. XRD analysis on the catalyst pellet after exposure to a reaction

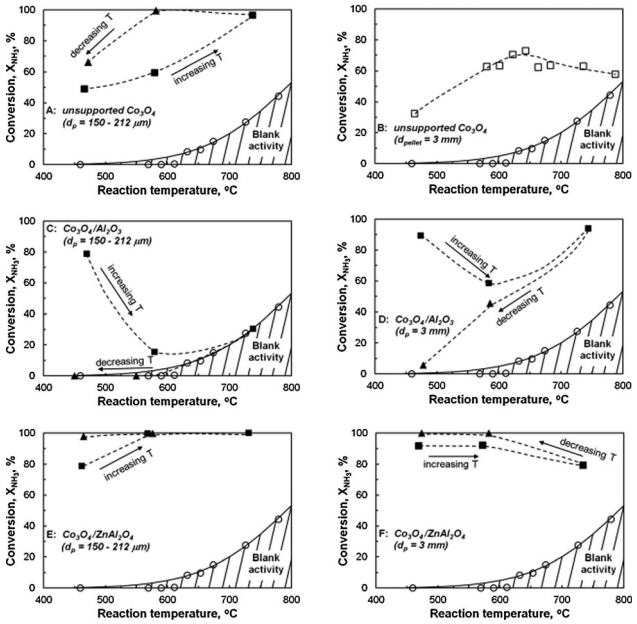

Fig. 2 Ammonia conversion over (un)supported Co_3O_4 as a function of the reaction temperature (A) unsupported Co_3O_4 (d_p = 150–212 μm), space velocity = 2.5 mmol NH_3 s^{-1} g^{-1}; (B) unsupported Co_3O_4 (d_p = 3 mm), space velocity = 0.2 mmol NH_3 s^{-1} g^{-1}; (C) Co_3O_4/Al_2O_3 (d_p = 150–212 μm), space velocity = 1.5 mmol NH_3 s^{-1} g^{-1}; (D) and (C) Co_3O_4/Al_2O_3 (d_p = 3mm), space velocity = 0.02 mmol NH_3 s^{-1} g^{-1}; (E) $Co_3O_4/ZnAl_2O_4$, space velocity = 1.5 mmol NH_3 s^{-1} g^{-1}; (F) $Co_3O_4/ZnAl_2O_4$ (d_p = 3 mm), space velocity = 0.02 mmol NH_3 s^{-1} g^{-1}.

Table 1 Characteristics of the fresh and spent Co_3O_4-pellets after exposure to ammonia oxidation conditions (crystal phase and average crystal size in the spent catalyst from Rietveld refinement of the powder XRD pattern)

	Fresh catalyst	Spent catalyst	
T_{max} (°C)	—	800	740
T_{final} (°C)	—	800	450
S_{BET} (m^2 g^{-1})	0.3	1.7	1.9
Co_3O_4 (wt%)	100	94.3 [b]	100 [b]
$d_{Co_3O_4}$	0.2–5[a] μm		
CoO (wt%)		5.7	—
d_{CoO} (nm)		27.4	—

[a] Determined using SEM. [b] Average crystallite size determination using Rietveld refinement not feasible.

temperature of 800 °C shows the presence of CoO (see Table 1) consistent with the thermodynamic analysis described above (the exit partial pressure of oxygen estimated under these conditions is *ca.* 0.1 bar). The presence of small CoO crystallites may indicate that these crystallites break-off from larger Co_3O_4 crystallites (a process driven by the density difference between Co_3O_4 and CoO[23]). Co(II)O can be re-oxidised under ammonia oxidation conditions by lowering the reaction temperature as shown by the disappearance of Co(II)O in the catalyst exposed to ammonia oxidation conditions at 450 °C after being exposed to 740 °C. The cleavage of small CoO crystallites, which are subsequently oxidised to Co_3O_4, results in a significant increase in the BET surface area and thus in a significant increase in the catalyst activity per unit mass.

The impregnation of cobalt nitrate on alumina (a mixture of γ-Al_2O_3, *ca.* 80 wt% and θ-Al_2O_3) resulted in small Co_3O_4 crystallites with an average size of *ca.* 8.4 nm (see Table 2). The ammonia conversion decreases with increasing temperature even going from 450 to 580 °C. The NH_3 conversion at a reaction temperature of 740 °C was equal to the ammonia conversion in the absence of the catalyst. Lowering the reaction temperature did not restore the catalyst activity.

Table 2 Characteristics of the fresh and spent supported Co_3O_4-pellets after the reversibility test (*i.e.* exposure to ammonia oxidation conditions at temperatures up to 740 °C and cooling down to 450 °C)

	Co_3O_4/Al_2O_3	$Co_3O_4/ZnAl_2O_4$
Fresh catalyst		
d_{pellet} (mm)	1 × 4	3 × 1
Co[a] (wt%)	9.0	8.4
S_{BET} (m^2 g^{-1})	196	24.3
Co_3O_4[b] (wt%)	13.4	7.4
$d_{Co_3O_4}$[b] (nm)	5.9	28.9
Spent catalyst		
S_{BET} (m^2 g^{-1})		19.1
Co_3O_4[b] (wt%)	5.9	10.3
$d_{Co_3O_4}$[b] (nm)	6.4	38.5
Co-support[b] (wt%)	3.1	—
$d_{Co\text{-}support}$[b] (nm)	15.6	—

[a] Determined using AAS-ICP. [b] Determined using Rietveld refinement of the powder XRD pattern.

The spent catalyst, both in pellet and in powder form, was dark blue in colour indicating the presence of cobalt aluminate in the sample. The formation of cobalt aluminate cannot be confirmed beyond doubt from the XRD analysis of the spent catalyst due to strongly overlapping diffraction peaks. Tentatively, *ca.* 10% of cobalt is present as XRD-visible cobalt aluminate. Furthermore, *ca.* 20% of cobalt has been transformed into XRD-invisible cobalt (possibly amorphous cobalt aluminate).

The formation of cobalt aluminate requires the presence of CoO,[17,18] which may react with alumina under hydrothermal conditions yielding cobalt aluminate. According to our thermodynamic analysis, neglecting the effect of crystallite size (which may become substantial in this size range[24]), Co_3O_4 crystallites with a diameter less than 6.0 nm maybe stable as CoO at temperatures as low as 560 °C at a partial pressure of O_2 of 0.1 bar. Crystallites with this diameter may be present in Co_3O_4/Al_2O_3, since the initial average crystallite diameter of Co_3O_4 was *ca.* 5.9 nm. The disappearance of small crystallites of Co_3O_4 from the crystallite size distribution is consistent with the slight increase in the average Co_3O_4 crystallite size observed. After exposure to high temperature ammonia oxidation conditions, the average crystallite size of Co_3O_4 in Co_3O_4/Al_2O_3 is slightly larger than in the fresh catalyst consistent with the conversion of small Co_3O_4 crystallites to Co(II)O.

The rapid diffusion of divalent cobalt into the alumina phase as demonstrated for γ-Al_2O_3 may lead to a cobalt-poor aluminate,[17] *i.e.* formation of XRD-amorphous cobalt aluminate with cobalt to aluminum ratio of less than 0.5. The location of the cobalt aluminate phase is currently unknown, but it may be associated with the cobalt oxide phase as suggested for the cobalt silicate formation,[25] since the reaction will also take place at the interface between CoO and alumina. This is further substantiated

by the lack of catalytic activity of Co_3O_4/Al_2O_3 after being exposed to a high reaction temperature, since the mere reduction in the surface area of Co_3O_4 would only account for a decrease in the activity by 60%. Hence, it is plausible that cobalt aluminate type of structures are covering the surface of Co_3O_4.

The synthesized zinc aluminate has relatively large crystallites of $ZnAl_2O_4$ and thus a relatively small surface area. The average pore radius in this support is estimated to be *ca.* 26 nm. The synthesized $Co_3O_4/ZnAl_2O_4$ contains relatively large Co_3O_4-crystallites with an average size of *ca.* 29 nm. It should however be noted that *ca.* 35% of cobalt seems to be XRD-invisible, which may be present as a highly dispersed phase on the $ZnAl_2O_4$ surface.

The ammonia conversion obtained over the $Co_3O_4/ZnAl_2O_4$ catalyst increases with increasing reaction temperature. Upon lowering the reaction temperature back to 450 °C, a higher conversion is obtained than the one originally obtained. Using $Co_3O_4/ZnAl_2O_4$ as a pellet introduced mass transfer limitations, and thus a lower activity than observed when using the catalyst in powder form. Upon increasing the temperature from 570 °C to 740 °C a decrease in the conversion of ammonia is observed. It is plausible that the deactivation is due to reduction of small crystallites of Co_3O_4 in the catalyst to CoO. The thermodynamic calculations indicate that Co_3O_4 crystallites with a diameter less than 18 nm are susceptible to reduction under the conditions applied. Upon decreasing the reaction temperature a higher activity is obtained showing that the observed deactivation is reversible.

The amount of XRD-invisible cobalt in the catalyst pellet is drastically reduced with *ca.* 10% of the cobalt remaining XRD-invisible. This is accompanied by an increase in the average crystallite size of Co_3O_4. The increase in the crystallite size can partially be explained by the reduction in the amount of XRD-invisible cobalt. Well-dispersed cobalt may migrate resulting in crystal growth. However, the change in the average crystallite size cannot solely be explained by the reduction in the amount of XRD-invisible cobalt indicating that some sintering is taking place as well.

The use of large crystallites of Co_3O_4 on a support would allow operation at a higher reaction temperature without the formation of CoO. High temperature may lead to a reversible type of deactivation (as observed for unsupported Co_3O_4 and pellets of $Co_3O_4/ZnAl_2O_4$ – see Fig. 1), since the formation of cobalt aluminate from CoO and zinc aluminate is thermodynamically not allowed,[26] even for nano-sized CoO crystallites if the surface energy of CoO is smaller than the surface energy of ZnO (γ_{ZnO}[27] = 1.42 J m^{-2}) assuming that the exchange reaction is not associated with simultaneous crystallite growth. The lack of incorporation of cobalt into the support makes zinc aluminate an ideal material as a washcoat to be applied in structured reactors or on foams, on which nano-crystallites of Co_3O_4 can be deposited.

The formation of cobalt aluminate is intrinsically linked to the ability to form CoO under reaction conditions.[18] The thermodynamic driving force for the formation of this phase can be linked to the crystallite size of the catalytically active phase. At this stage it is not clear whether the reduction or the re-oxidation is the size dependent step. This can only be evaluated using catalysts with well-defined crystallite size distributions.[28] Supporting these well-defined crystallites on the selected support materials would allow further insights into the deactivation behavior of this type of catalysts.

Conclusions

Co_3O_4-containing ammonia oxidation catalysts may undergo a reduction to CoO in the presence of oxygen at high temperature. Nano-sized Co_3O_4 crystallites are more susceptible to the reduction reaction in the presence of oxygen, if the surface energy of CoO is lower than the surface energy of Co_3O_4. The reduction of Co_3O_4 represents a reversible deactivation, since lowering the reaction temperature will result in the re-oxidation of CoO. However, CoO can further react under the hydrothermal conditions of ammonia oxidation with support materials, such as alumina, yielding cobalt aluminate, which may adhere to cobalt oxide reducing the catalytically active surface area accessible to the reactants. The reaction between CoO and $ZnAl_2O_4$ is thermodynamically not allowed, making zinc aluminate an ideal support material for Co_3O_4 as a catalyst for ammonia oxidation.

Notes and references

1 S. I. Clarke and W. J. Mazzaro, *Nitric acid*, *Kirk–Othmer Encyclopedia of Chemical Technology*, 2005, vol. 17, pp. 1–17.
2 V. Sadykov, L. Isupova, I. Zolotarskii, L. Bobrova, A. Noskov, V. Parmon, E. Brushtein, T. Telyatnikova, V. Chernyshev and V. Lunin, *Appl. Catal., A*, 1975, **39**, 73.
3 N. II'chenko, *J. Catal.*, 1975, **39**, 73; N. II'chenko and G. I. Golodets, *Russ. Chem. Rev.*, 1976, **45**, 2168; K. Schmidt-Szalowski, K. Krawczyk and J. Petryk, *Appl. Catal., A*, 1998, **175**, 147.
4 C. R. Maxwell, *Synthetic nitrogen products: a practical guide ot products and process*, Kluwer Academic/Plenum Press, New York, 2004.
5 J. Pérez-Ramírez and E. Kondratenko, *J. Catal.*, 2007, **250**, 240.
6 G. Biausque and Y. Schuurman, *J. Catal.*, 2010, **276**, 306.
7 Y. Wu, T. Yu, B.-S. Cou, C.-X. Wang, X. F. Xie, Z.-L. Yu, S.-R. Fan and L.-C. Wang, *J. Catal.*, 1989, **120**, 88; S. Ramesh, S. S. Manharan, M. S. Hedge and K. C. Patil, *J. Catal.*, 1995, **157**, 749.
8 J. Pérez-Ramírez and B. Vigeland, *Catal. Today*, 2005, **105**, 436; S. Sun, M. Rebeilleau-Dassonneville, X. Zhu, W. Chu and W. Yang, *Catal. Today*, 2010, **149**, 167.
9 E. van Steen, M. Claeys, M. E. Dry, J. van de Loosdrecht, E. L. Viljoen and J. L. Visagie, *J. Phys. Chem. B*, 2005, **109**, 3575.
10 A. Navrotsky, C. Ma, K. Lilova and N. Birkner, *Science*, 2010, **220**, 199.
11 F. Zasada, W. Piskorz, P. Stelmachowski, A. Kotarba, J.-F. Paul, T. Płociński, K. J. Kurzydłowski and Z. Soika, *J. Phys. Chem. C*, 2011, **115**, 6423.

12 L. Wang, K. Vu, A. Navrotsky, R. Stevens, B. F. Woodfield and J. Boerio-Goates, *Chem. Mater.*, 2004, **16**, 5394.
13 J. C. W. Swart, PhD thesis, University of Cape Town, 2008.
14 G. S. Sewell, E. van Steen and C. T. O'Connor, *Catal. Lett.*, 1996, **37**, 255.
15 W.-K. Fung, M. Claeys and E. van Steen, *Catal. Lett.*, 2012, **142**, 445.
16 S. Roy, A. K. Heibel, W. Liu and T. Boger, *Chem. Eng. Sci.*, 2004, **59**, 957; M. Estenfelder and A. Cremona, *US Patent*, 0158784 A1, 2010.
17 P. H. Bolt, F. H. P. M. Habraken and J. W. Geus, *J. Solid State Chem.*, 1998, **135**, 59.
18 P. J. van Berge, J. van de Loosdrecht, S. Barradas and A. M. van der Kraan, *Catal. Today*, 2000, **58**, 321; G. Kiss, C. E. Kliewer, G. J. DeMartin, C. C. Culross and J. E. Baumgartner, *J. Catal.*, 2003, **217**, 127; A. Sirijaruphan, A. Horváth, J. G. Goodwin Jr. and R. Oukaci, *Catal. Lett.*, 2003, **91**, 89.
19 S. Farhadi and S. Panahandehjoo, *Appl. Catal., A*, 2010, **382**, 293; A 25 wt% aqueous NH_3 solution was added drop-wise to an aqueous solution containing 43 mmol L^{-1} $Al(NO_3)_3{\cdot}9H_2O$ and 21.5 mmol L^{-1} $Zn(CH_3COO)_2$ to obtain a pH of 9. The resulting slurry was subsequently aged for 1 h at room temperature. The solid was filtered off, dried overnight at 120 °C, and further calcined in air at 800 °C for 4 h.
20 Y. Q. Zhuang, M. Claeys and E. van Steen, *Appl. Catal., A*, 2006, **301**, 138.
21 R. J. Berger, J. Pérez-Ramírez, F. Kapteijn and J. A. Moulijn, *Chem. Eng. J.*, 2002, **90**(2002), 173.
22 I. Vogel, *Determination of ammonia*, *Quantitative Inorganic Analysis*, John Wiley & Sons, New York, 1961, 3rd edn, pp. 783–785.
23 M. M. Hauman, A. Saib, D. J. Moodley, M. Claeys and E. van Steen, *ChemCatChem*, 2012, **4**, 1411.
24 J. C. W. Swart, P. van Helden and E. van Steen, *J. Phys. Chem. C*, 2007, **111**, 4998.
25 D. Potoczna-Petru and L. Krajczyk, *Catal. Lett.*, 2003, **87**, 51.
26 O. Knacke, O. Kubaschewski and K. Hesselmann, *Thermochemical properties of inorganic substances*, Springer Verlag, Berlin, 2nd edn, 1991.
27 F. Xu, P. Zhang, A. Navrotsky, Z.-Y. Yuan, T.-Z. Ren, M. Halasa and B.-L. Su, *Chem. Mater.*, 2007, **19**, 5680.
28 N. Fischer, E. van Steen and M. Claeys, *Catal. Today*, 2011, **171**, 327.